A Tale of Two Regions: A Mathematical Model for Chagas' Disease

Alhaji Cherif[1]
Viviana García Horton[2]
Glorimar Meléndez Rosario[3]
William Feliciano[3]
Britnee Crawford[4]
José Vega Guzmán[5]
Fabio Sánchez[6]

Christopher Kribs-Zaleta[4]

[1] Theoretical and Applied Mechanics, Cornell University

[2] Departamento de Matemáticas, Instituto Tecnológico Autónomo de México

[3] Departamento de Matemática-Física, Universidad de Puerto Rico-Cayey

[4] Department of Mathematics, University of Texas-Arlington

[5] Department of Mathematics and Statistics, Arizona State University

[6] OPEN Risk Management Team, American Express, Inc.

Abstract

We model the epidemiological interactions between two animal populations: one with a virulent strain of *Trypanosoma cruzi*, which causes Chagas' disease, and the other with a non-virulent strain that provides cross immunity against the disease. The virulent strains of *T. cruzi* are predominantly found in Latin America. The increased spread of Chagas' disease from its endemic habitat in Latin America to the north, which has recently been observed, has been linked to climate change and deforestation. As a result, a large part of the southern United States is at a higher risk for the disease. The two-patch model presented herein describes the effects of the migrating virulent strains on the prevalence and/or possibility of endemicity of Chagas' disease in the United States. We use an epidemiological modelling paradigm and an analytical framework of nonlinear dynamics to describe the behavior of the two populations and their interactions. Depending on certain conditions imposed on reproductive numbers, we found that there are six different scenarios for the two-patch system as a whole. We found that the principle of competitive exclusion prevails in either strain when there is no migration, with the exception of infinitely many stable non-isolated steady states of coexistence on the bifurcation line in the $R_{21} - R_{22}$ plane. When the migration term is nonzero, we observed that there are two possible situations for patch 2: endemic equilibrium for the virulent strain or coexistence of both strains.

A Introduction

Chagas' disease is a vector-borne parasitic disease that predominantly affects Latin American countries. *Trypanosoma cruzi*, the parasite responsible for Chagas', can be found over a wide area of the American continent, from the southern half of the United States to Chile and central Argentina, in a total of 18 countries [7]. Approximately 90 million people are at risk of infection in countries like Mexico and Brazil, and it is estimated to affect between 16 and 18 million people. Cases of endemic breakout have been confined mainly to Latin America (specifically, the rural areas and tropical regions).

Chagas' disease results from infection with the protozoan parasite *Trypanosoma cruzi*, a member of the order *Kinetoplastida* and family *Trypanosomatidae*. There exist many strains of *T. cruzi* classified primarily under two classes: *T. cruzi I* and *T. cruzi II*. The former, native to Mexico, causes Chagas' disease; the latter, found mostly in southern United States, does not cause any pathology but provides cross-immunity against the first one [2]. For expository purposes only, we refer to the strain that causes Chagas' disease as *T. cruzi* strain 1 (or chagasic/virulent), and name the strain that provides cross-immunity *T. cruzi* strain 2 (or non-chagasic/non-virulent).

The most common method of infection is through blood-feeding insects under the genus *Triatoma*, *Rhodnius*, and *Panstrongylus*, which act as vectors. Triatoma are generally large, measuring about 35 mm in length. The life cycle of Triatoma initially starts at immature nymphal stage, and is divided into five nymphal stages with no pupal stage. It has been observed that Triatoma's hatch-rate is temperature sensitive. They usually hatch after ten to forty days, and after hatching they generally feed on a host within two to three days. If no host is available, a nymph can survive several weeks before actually feeding. Females lay 100-600 eggs during their three to twelve month lifespan. The reproductive capacity of the adult male has been observed to be temperature sensitive due to the fact that at low temperature the male cannot fertilize eggs, which are usually laid in small clumps in arboreal environments. For instance, two generations of egg development may be completed per year in warmer climates, whereas one generation is completed in colder climates. During developmental stage, a large blood-meal is required, which consists of 1-2 grams blood on average and lasts for 14 days.

These bugs are often found in cracks, roofs and crevices of houses that are poorly constructed, mostly in rural areas, and they are known to feed on the blood of the infected and/or potential hosts or reservoirs. However, the infection is transmitted when the insect defecates near the wound of the potential host. In most cases, the parasites contained in the feces of the insect penetrate the skin through wounds resulting from scratching [6]. Researchers have found that infected vectors sometime change their behavior [3]. The most important differential behavior is the modification of their eating habits. For instance, the parasites hamper the vectors' ability to draw blood efficiently, compelling them to feed more often than uninfected vectors. These changes in the vectors' habits provide biological justification for the increase in their mobility, hence increasing the infection rate [3, 16].

There are more than 100 species of mammals that can serve as hosts for *Trypanosoma cruzi*. In the United States, the most frequent are opossums, rats, armadillos, raccoons, woodrats, mice, dogs, and cats, among others [8]. All the stages of Chagas' disease are known to occur in dogs, but it has rarely been described in cats, for

example. There is little information about the actual Chagas' disease in other species; however, it is known that mammals like raccoons and opossums act as reservoirs for *T. cruzi* [8], which means that they are carriers of the parasite but are not themselves affected with the disease.

From a medical perspective, the disease has an incubation period ranging from 5 to 14 days after exposure to the vector's feces. The human disease occurs mainly in two stages: the acute stage shortly after the infection, and the chronic stage that may develop over about 5 to 40 years later [8]. The acute infection phase lasts 2 to 3 months and is often mild; usually a small sore develops at the bite where the parasite enters the body. Within a few days, fever and swollen lymph nodes may develop. This initial acute phase may cause illness and death, especially in young children. An estimated 30% of infected people will develop medical problems from Chagas' disease over the course of their lives, and will not become symptomatic until the chronic stage. During this period of time, parasites are invading most organs of the body, often causing heart, intestinal and oesophageal damage and progressive weakness. Complications of chronic Chagas' disease may include organ failure, usually of the heart or digestive system, due to secondary fibrosis [8].

The finding about strain 2 of *T. cruzi* providing cross-immunity against strain 1 has been supported by an experiment on mice described in [1]. It was shown that mice infected with the virulent strain responded to the disease drastically and died in the following day, while mice infected with the non-virulent one showed no sign of the disease. L. Lauria-Pires et al. [1] discovered that co-infection between the strains is not permitted when mice previously infected with nonvirulent strain were later reinfected with the virulent strain. However, they found that both strains were present in their blood work [1]. As a result, scientists and researchers investigating this effect have come to believe that *T. cruzi* 2 could provide immunization against Chagas' disease [8].

Propagation of vector-borne diseases such as Chagas' has been known to be strongly influenced by a number of environmental factors such as temperature, vegetation, and host species. The increased spread of Chagas' disease from its endemic habitat in Latin America to the north, which has recently been observed, has been linked to climate change (such as higher temperatures) and deforestation. These factors could extend the geographical distribution of the vectors, putting a large part of the southern United States at increased risk for the disease. Also, this higher risk range is expected to extend into the central United States in the next twenty years because of the rising temperatures which have been predicted [34]. These facts serve as motivation for the present study, where we focus on modelling the interaction of two strains of *T. cruzi* in two different populations, and the effects that migration can produce in the dynamics of such populations.

Recently, researchers from various disciplines have developed multiple models describing and capturing the dynamics of transmission. Many of the papers that have appeared focus on the spread of Chagas' disease, vector consumption and contact dynamics, differential behavior in the vectors experiencing different environmental conditions [2, 3]. In [2], the contributions made by the vector consumption and contact process saturation in sylvatic transmission of *T. cruzi* strain were investigated using the basic reproductive number as a comparison metric. Recent investigations [4] have shown the coexistence of both strains of *T. cruzi* in some habitats in the United States, where the native strain provides cross-immunity against the virulent one.

The model presented herein studies the interaction of two populations infected with *T.cruzi*, considering as well two different strains of the parasite, and in the presence of one-directional vector migration (asymmetric migration). An epidemiological framework and tools from nonlinear dynamics are used to gain insight into the dynamics of the system under consideration (e.g. the dominance of one strain of *T. cruzi* over another). This study is of great importance to the United States and many Latin American countries, and provides initial steps toward the development of diagnostic and preventive policies for Chagas' disease. The rest of the paper is divided as follows: section 2 presents a model which describes the interaction between the two strains; section 3 discusses relevant analysis of the model; section 4 provides parameter estimations and numerical simulations of the model. The paper ends with a conclusion, which summarizes the main results and provides future direction.

B Proposed model

We develop a model to analyze *T. cruzi* infection, in which we consider two distinct patches that differ in the kind of strain of *T. cruzi* that is present. We divide the total population into hosts and vectors, and consider for both of these groups the individuals who are susceptible to infection by *T. cruzi* (denoted by S) and those who have been in contact with the parasite and have it present in their bloodstream (denoted by I). We consider that the host population consists of raccoons and opossums, which act as reservoirs for the parasite. In addition, the vector population are bugs of the genus Triatoma, including *Triatoma sanguisuga* and *Triatoma dimidiata*, which are amongst the most important vectors for *T. cruzi* in Mexico and the U.S.

We consider that the infected individuals in patch 1 (both hosts and vectors) only have the virulent strain,

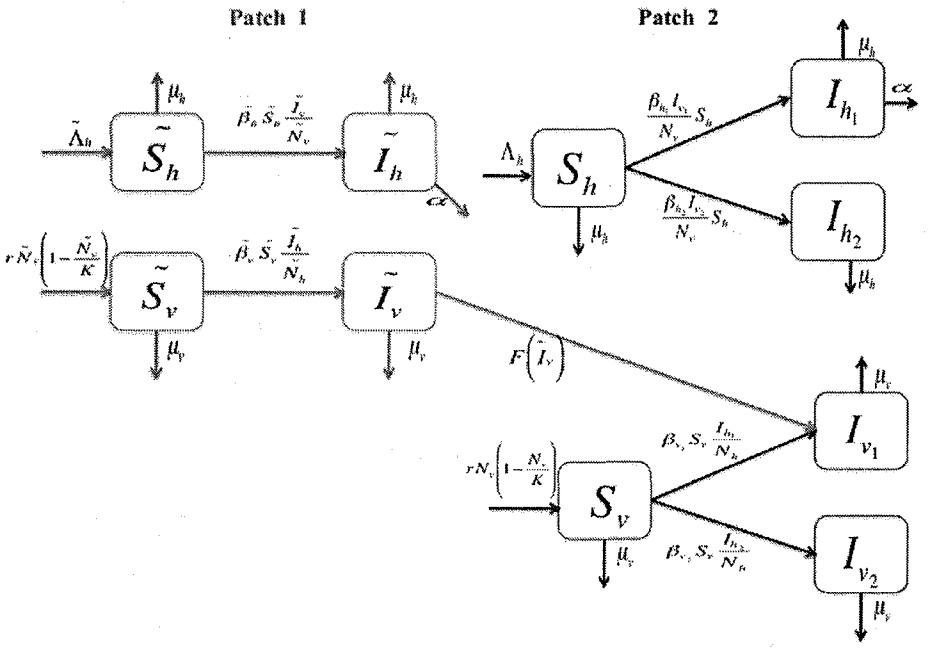

Figure 27: Two patch model for Chagas' disease

while in patch 2 they have either the non-virulent strain or, as a result of migration from patch 1, the virulent strain. However, in patch 2 the prevalence of the virulent strain is much smaller than that of the non-virulent strain. We then incorporate an asymmetric migration term, in which a proportion of the infected vectors from patch 1 move to patch 2. We make the assumption that only infected vectors migrate due to the fact that the chagasic vectors have differential eating behaviors, as was mentioned before. With this assumption, both strains of *T. cruzi* will be present in patch 2, while in patch 1 there will only be a presence of the virulent strain; this is, the analysis of patch 2 will provide us with the means for studying the existence of the cross-immunity phenomenon.

The parameters of the model are given in Table 14. The subscripts h and v are used to denote hosts and vectors, respectively, and the numbers 1 or 2 denote the *T. cruzi* strain type present in the individual. In particular, we use 1 for the virulent strain and 2 for the non-virulent strain. We are also using a tilde ($\tilde{}$) for all the elements in patch 1. The letter N refers to the total population.

The equations describing the system in patch 1 are given as follows:

$$\begin{aligned}
\frac{d\tilde{S}_h}{dt} &= \tilde{\Lambda}_h - \tilde{\beta}_h \tilde{S}_h \frac{\tilde{I}_v}{\tilde{N}_v} - \mu_h \tilde{S}_h \\
\frac{d\tilde{I}_h}{dt} &= \tilde{\beta}_h \tilde{S}_h \frac{\tilde{I}_v}{\tilde{N}_v} - \mu_h \tilde{I}_h - \alpha \tilde{I}_h \\
\frac{d\tilde{S}_v}{dt} &= r\tilde{N}_v \left(1 - \frac{\tilde{N}_v}{K}\right) - \tilde{\beta}_v \tilde{S}_v \frac{\tilde{I}_h}{\tilde{N}_h} - \mu_v \tilde{S}_v \\
\frac{d\tilde{I}_v}{dt} &= \tilde{\beta}_v \tilde{S}_v \frac{\tilde{I}_h}{\tilde{N}_h} - \mu_v \tilde{I}_v - F\left(\tilde{I}_v\right)
\end{aligned}$$

In the equations above, $\tilde{\Lambda}_h$ represents the recruitment rate of hosts, and $\tilde{\beta}_h$ and $\tilde{\beta}_v$ are the per capita host and vector infection rates, respectively. The only transmission method that is taken into account is horizontal transmission (resulting from bites). μ_h and μ_v are the per capita natural death rates. We assume μ_h to be the same for both patches, and similarly for μ_v, because we are not taking into account the differences in environmental conditions between the two patches which may produce changes in the life span of either hosts or vectors. The constant α is the disease-induced mortality rate, which changes considerably depending on the type of host. For instance, in the case of mice this term is significant because they die of the disease in a short period of time; however, raccoons just act as host-reservoirs, which means they don't contract the disease so this term is negligible. As a result, in the particular case that we are analyzing the disease-induced mortality rate will be zero because the raccoons and opossums (reservoirs) do not die from Chagas' disease. However, we choose to do all the analysis including the α so that the model can be useful for further research, for example when considering mice and dogs (that do die from the disease) or even humans (in a very long period of time) as hosts.

The nonlinear terms in the equations above account for the contacts between hosts and vectors which result in an infection. The term $F\left(\tilde{I}_v\right)$ corresponds to the migration of infected vectors from patch 1 (chagasic) to patch 2. For simplicity, linear migratory function is considered, i.e. of the form

$$F\left(\tilde{I}_v\right) = m\tilde{I}_v$$

for some per capita migration constant m. In this patch, we have the total populations

$$\begin{aligned} \tilde{N}_h &= \tilde{S}_h + \tilde{I}_h \\ \tilde{N}_v &= \tilde{S}_v + \tilde{I}_v \end{aligned}$$

In the case of patch 2 there will be six equations, because we take into consideration susceptible hosts and

Notation	Definition
$\tilde{\Lambda}_h$	Recruitment rate for hosts in patch 1
$\tilde{\beta}_h$	Infection rate for hosts in patch 1
μ_h	Death rate for hosts
α	Disease-induced mortality rate
r	Growth rate for vector population
K	Carrying capacity of the vector population
$\tilde{\beta}_v$	Infection rate for vectors in patch 1 (virulent strain)
Λ_h	Recruitment rate for hosts in patch 2
μ_v	Death rate for vectors
β_{h1}	Rate of infection with non-virulent strain for hosts in patch 2
β_{h2}	Rate of infection with virulent strain for hosts in patch 2
β_{v1}	Rate of infection with non-virulent strain for vectors in patch 2
β_{v2}	Rate of infection with virulent strain for vectors in patch 2

Table 14: Parameters of the model

vectors, as well as infected hosts and vectors with each of the two strains. The system is as follows:

$$\begin{aligned}
\frac{dS_h}{dt} &= \Lambda_h - S_h\left(\frac{\beta_{h1}I_{v1}+\beta_{h2}I_{v2}}{N_v}\right) - \mu_h S_h \\
\frac{dI_{h1}}{dt} &= \beta_{h1}S_h\frac{I_{v1}}{N_v} - \mu_h I_{h1} - \alpha I_{h1} \\
\frac{dI_{h2}}{dt} &= \beta_{h2}S_h\frac{I_{v2}}{N_v} - \mu_h I_{h2} \\
\frac{dS_v}{dt} &= rN_v\left(1-\frac{N_v}{K}\right) - S_v\left(\frac{\beta_{v1}I_{h1}+\beta_{v2}I_{h2}}{N_h}\right) - \mu_v S_v \\
\frac{dI_{v1}}{dt} &= \beta_{v1}S_v\frac{I_{h1}}{N_h} - \mu_v I_{v1} + F\left(\tilde{I}_v\right) \\
\frac{dI_{v2}}{dt} &= \beta_{v2}S_v\frac{I_{h2}}{N_h} - \mu_v I_{v2}
\end{aligned}$$

with the total populations satisfying

$$\begin{aligned}
N_h &= S_h + I_{h1} + I_{h2} \\
N_v &= S_v + I_{v1} + I_{v2}
\end{aligned}$$

The basic notation in this patch is the same as before.

The total vector population is not constant in either patch, because patch 1 is losing individuals to migration whereas patch 2 is gaining them. We include a logistic growth for the vector population to account for the change in population due to migration. In this expression, r is the growth rate and K the carrying capacity of the vectors.

We choose to include constant recruitment rate for hosts because we include the possibility of having hosts coming in from nearby locations as well as the intrinsic growth pertaining to the local population. For the vectors, we assume logistic growth so that we only have the intrinsic growth for this population, and this way we do not consider vectors coming from different locations.

Due to the functional form of the migratory term and its asymmetric nature, the system of equations in patch 1 is decoupled from those in patch 2. This enables us to analyze the system in patch 1 easily and use the endemic equilibrium obtained to analyze the behavior of patch 2.

C Analysis

In this section, we perform the analysis of the model proposed previously. Since the the first patch is decoupled from the second patch, we will first analyze it without considering the effect of migration. The scheme of the analysis of the model is as follows: the first subsection focuses on the analysis of patch 1 in isolation (where $m = 0$); the second provides analysis on patch 2, again assuming $m = 0$; finally we study both patches taking into account the dynamics of migration.

C.1 Patch 1 (no migration)

First of all we consider, for demographic purposes, the behavior of the total population of vectors with respect to the parameters used to define their growth rate (r) and their natural death rate (μ_v). With this, we can derive a demographic condition under which the vectors would go extinct, which would imply that there are no infections and migration could not possibly exist. This condition gives that whenever r is less than μ_v, the population of vectors goes extinct. Therefore, in the following analysis we will assume that r is greater than μ_v.

The population of susceptible vectors persists if and only if the intrinsic growth rate of the vector population (r) is greater than the natural death rate μ_v.

Proof. We use the equation for the total population of vectors

$$\frac{d\tilde{N}_v}{dt} = f\left(\tilde{N}_v\right) = r\tilde{N}_v\left(1-\frac{\tilde{N}_v}{K}\right) - \mu_v\tilde{N}_v$$

and look at its stability, not considering migration. The fixed points are $\tilde{N}_v^* = 0, \tilde{N}_v^* = K\left(1 - \frac{\mu_v}{r}\right)$. We take the derivative with respect to $\tilde{N}_v$:

$$f'\left(\tilde{N}_v\right) = r - \frac{2r\tilde{N}_v}{K} - \mu_v$$

For the fixed point $\tilde{N}_v^* = 0$, we have that $f' > 0 \Leftrightarrow r > \mu_v$, which implies that there is no extinction since $\tilde{N}_v^* = 0$ is unstable. For $\tilde{N}_v^* = K\left(1 - \frac{\mu_v}{r}\right)$, we have $f' < 0 \Leftrightarrow r > \mu_v$, which implies that the fixed point is stable. □

The first step of the analysis consisted in calculating the basic reproductive number R'_{10} using the next generation operator approach [10]. We obtained as a result the following expression:

$$R'_{10} = \sqrt{\frac{\tilde{\beta}_h}{(\mu_h + \alpha)} \frac{\tilde{\beta}_v}{\mu_v}}.$$

R'_{10} can be interpreted as the geometric mean of the average number of secondary vector infections produced by one infected host, and the average number of secondary host infections produced by one infected vector.

Next, we calculate the fixed points. For this particular case, we obtained two: the infection-free equilibrium (denoted by E_{10}), which occurs when $\tilde{I}_h^* = 0$ and $\tilde{I}_v^* = 0$, and the endemic equilibrium (E'_{11}). Due to structural complexity, we proportionalize the steady state conditions using the following:

$$\tilde{S}_h^* = (1 - x_h)\tilde{N}_h^* \quad (85)$$
$$\tilde{I}_h^* = x_h\tilde{N}_h^* \quad (86)$$
$$\tilde{S}_v^* = (1 - x_v)\tilde{N}_v^* \quad (87)$$
$$\tilde{I}_v^* = x_v\tilde{N}_v^* \quad (88)$$

In the case of the infection-free equilibrium (E_{10}), we have $\tilde{S}_h^* = \tilde{N}_h^*$ and $\tilde{S}_v^* = \tilde{N}_v^*$. Thus, E_{10} is given by

$$E_{10} : \left(\tilde{S}_h^*, \tilde{I}_h^*, \tilde{S}_v^*, \tilde{I}_v^*\right) = \left(\frac{\tilde{\Lambda}_h}{\mu_h}, 0, \frac{K\left(r - \mu_v\right)}{r}, 0\right)$$

The existence of this equilibrium is easily shown because of the fact that $\tilde{\Lambda}_h, \mu_h, K, r > 0$ and $r - \mu_v > 0$ as well.

To obtain the endemic equilibrium, we use equations (1-4) and replace the steady state conditions for $\tilde{S}_h^*$ and $\tilde{S}_v^*$ with the steady state conditions for $\tilde{N}_h^*$ and $\tilde{N}_v^*$, respectively, and solve for $\tilde{N}_h^*, \tilde{N}_v^*, x_h$, and x_v. This way, we obtain the endemic equilibrium (E'_{11}), which is given by:

$$E'_{11} : \begin{pmatrix} 1 - x_h \\ x_h \\ 1 - x_v \\ x_v \end{pmatrix} = \begin{pmatrix} \frac{1}{R'^2_{10}} + \left(1 - \frac{1}{R'^2_{10}}\right)\left(\frac{\mu_h + \alpha}{\tilde{\beta}_h + \mu_h + \alpha}\right) \\ \left(1 - \frac{1}{R'^2_{10}}\right)\left(\frac{\tilde{\beta}_h}{\tilde{\beta}_h + \mu_h + \alpha}\right) \\ \frac{1}{R'^2_{10}} + \left(1 - \frac{1}{R'^2_{10}}\right)\left(\frac{\mu_v}{\tilde{\beta}_v + \mu_v}\right) \\ \left(1 - \frac{1}{R'^2_{10}}\right)\left(\frac{\tilde{\beta}_v}{\tilde{\beta}_v + \mu_v}\right) \end{pmatrix}$$

where

$$\tilde{N}_h^* = \frac{\Lambda}{\mu_h + \alpha x_h}$$
$$\tilde{N}_v^* = K\left(1 - \frac{\mu_v}{r}\right)$$

where R'_{10} is the basic reproductive number for this patch. Using the basic reproductive number R'_{10}, we were able to prove the existence of the endemic equilibrium (E'_{11}) by showing that each of the coordinates is positive when $R'_{10} > 1$.

R'_{10} can also be used to provide insight into the dynamics of the system and to study the stability of the infection-free equilibrium. When $R'_{10} < 1$, the infection-free equilibrium E_{10} is locally stable, and $R'_{10} > 1$ implies that the infection-free equilibrium is unstable and allows the possibility of having an endemic equilibrium that is stable. In other words, the condition for the existence of endemicity is given by $R'_{10} > 1$. It can be seen that an exchange of stability between E_{10} and E'_{11} occurs at the threshold value $R'_{10} = 1$ through a transcritical bifurcation (see Figure 28).

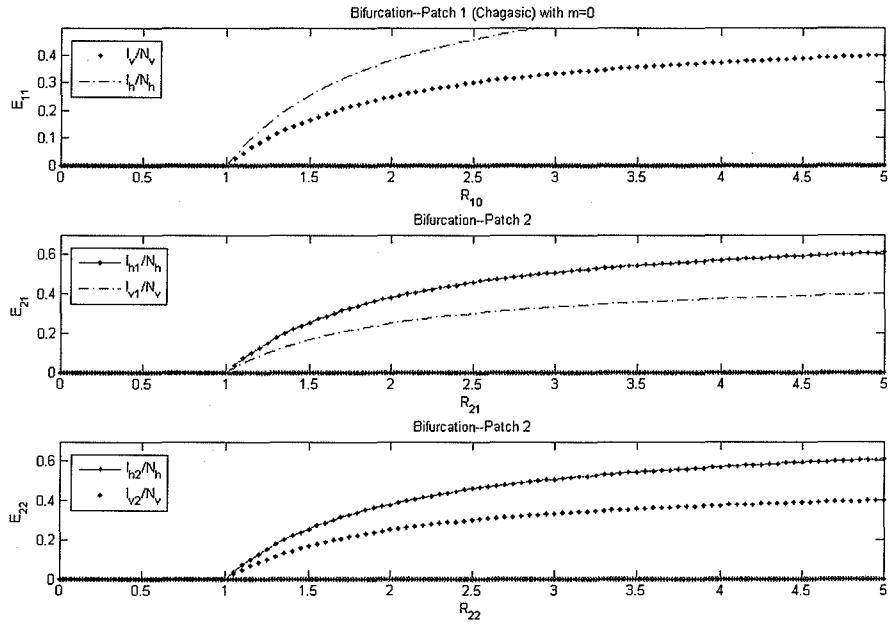

Figure 28: Transcritical Bifurcations

It can in fact be shown that the infection-free equilibrium is globally asymptotically stable if we impose the condition that $R'_{10} \leq 1$. To prove this, the condition is restated in the following proposition:

The infection-free equilibrium E_{10} is globally stable in patch 1 with $m = 0$ if $R'_{10} \leq 1$.

Proof. We will use the integro-differential equation method [29], often called "a priori estimates" to prove global stability for E'_{10} when $R'_{10} < 1$. It is sufficient to show that the solutions for $\tilde{S}_v$ and $\tilde{S}_h$ are bounded and that $\tilde{I}_h$ and $\tilde{I}_v$ go to zero. From the original equations:

$$\begin{aligned} \frac{d\tilde{I}_h}{dt} &= \tilde{\beta}_h \tilde{S}_h \frac{\tilde{I}_v}{\tilde{N}_v} - \mu_h \tilde{I}_h - \alpha \tilde{I}_h \\ \frac{d\tilde{I}_v}{dt} &= \tilde{\beta}_v \tilde{S}_v \frac{\tilde{I}_h}{\tilde{N}_h} - \mu_v \tilde{I}_v - F\left(\tilde{I}_v\right) \end{aligned}$$

By integrating, we get

$$\tilde{I}_h(t) \leq I_0 e^{-(\mu_h+\alpha)t} + \tilde{\beta}_h \int_0^t e^{(\mu_h+\alpha)(\tau-t)} \tilde{S}_h(\tau) \frac{\tilde{I}_v(\tau)}{\tilde{N}_v(\tau)} d\tau$$

Dividing by $\tilde{N}_h(t)$

$$\frac{\tilde{I}_h(t)}{\tilde{N}_h(t)} \leq \frac{I_0}{\tilde{N}_h} e^{-(\mu_h+\alpha)t} + \frac{\tilde{\beta}_h}{\tilde{N}_h} \int_0^t e^{(\mu_h+\alpha)(\tau-t)} \tilde{S}_h(\tau) \frac{\tilde{I}_v(\tau)}{\tilde{N}_v(\tau)} d\tau$$

So by taking $\limsup_t$ in both sides

$$\begin{aligned} \limsup_t \frac{\tilde{I}_h(t)}{\tilde{N}_h(t)} &\leq \limsup_t \left(\frac{I_0}{\tilde{N}_h(t)} e^{-(\mu_h+\alpha)t} + \frac{\tilde{\beta}_h}{\tilde{N}_h(t)} \int_0^t e^{(\mu_h+\alpha)(\tau-t)} \tilde{S}_h(\tau) \frac{\tilde{I}_v(\tau)}{\tilde{N}_v(\tau)} d\tau \right) \\ &\leq \limsup_t \frac{\tilde{\beta}_h}{\tilde{N}_h(t)} \int_0^t e^{(\mu_h+\alpha)(\tau-t)} \tilde{S}_h(\tau) \frac{\tilde{I}_v(\tau)}{\tilde{N}_v(\tau)} d\tau \end{aligned}$$

because $\limsup_t I_0 e^{-(\mu_h+\alpha)t} = 0$. Let $x = t - \tau \Rightarrow \tau = t - x$. Then

$$\begin{aligned}\limsup_t \frac{\tilde{I}_h(t)}{\tilde{N}_h(t)} &\leq \limsup_t \frac{\tilde{\beta}_h}{\tilde{N}_h(t)} \int_0^t e^{-(\mu_h+\alpha)x} \tilde{S}_h(t-x) \frac{\tilde{I}_v(t-x)}{\tilde{N}_v(t-x)} dx \\ &\leq \tilde{\beta}_h \int_0^t \left(\limsup_t e^{-(\mu_h+\alpha)x} \limsup_t \frac{\tilde{S}_h(t-x)}{\tilde{N}_h(t)} \frac{\tilde{I}_v(t-x)}{\tilde{N}_v(t-x)} \right) dx\end{aligned}$$

where the second inequality is given by the Fatou-Lebesgue Theorem. Using the definition

$$\limsup_t f(t-x) = \limsup_t f(t)$$

we get

$$\begin{aligned}\limsup_t \frac{\tilde{I}_h(t)}{\tilde{N}_h(t)} &\leq \frac{\tilde{\beta}_h}{\mu_h+\alpha} \limsup_t \frac{\tilde{S}_h(t)}{\tilde{N}_h(t)} \frac{\tilde{I}_v(t)}{\tilde{N}_v(t)} \\ &\leq \frac{\tilde{\beta}_h}{\mu_h+\alpha} \limsup_t \frac{\tilde{S}_h(t)}{\tilde{N}_h(t)} \limsup_t \frac{\tilde{I}_v(t)}{\tilde{N}_v(t)}\end{aligned}$$

We know that

$$\begin{aligned}\tilde{N}_h &= \tilde{S}_h + \tilde{I}_h, \tilde{N}_v = \tilde{S}_v + \tilde{I}_v \\ &\Rightarrow \tilde{S}_h \leq \tilde{N}_h, \tilde{I}_h \leq \tilde{N}_h, \tilde{S}_v \leq \tilde{N}_v, \tilde{I}_v \leq \tilde{N}_v\end{aligned}$$

and

$$\frac{\tilde{S}_h}{\tilde{N}_h} \leq 1, \frac{\tilde{S}_v}{\tilde{N}_v} \leq 1$$

so

$$\limsup_t \frac{\tilde{S}_h(t)}{\tilde{N}_h(t)} \leq \sup_t \frac{\tilde{S}_h(t)}{\tilde{N}_h(t)} = 1$$

Finally we obtain

$$\limsup_t \frac{\tilde{I}_h(t)}{\tilde{N}_h(t)} \leq \frac{\tilde{\beta}_h}{\mu_h+\alpha} \limsup_t \frac{\tilde{I}_v(t)}{\tilde{N}_v(t)}$$

Similarly we obtain

$$\limsup_t \frac{\tilde{I}_v(t)}{\tilde{N}_v(t)} \leq \frac{\tilde{\beta}_v}{\mu_v} \limsup_t \frac{\tilde{I}_h(t)}{\tilde{N}_h(t)}$$

since they have the same structure. Substituting the second expression into the first, we get

$$\limsup_t \frac{\tilde{I}_h(t)}{\tilde{N}_h(t)} \leq \frac{\tilde{\beta}_h}{\mu_h+\alpha} \frac{\tilde{\beta}_v}{\mu_v} \limsup_t \frac{\tilde{I}_h(t)}{\tilde{N}_h(t)} = R_{10}'^2 \limsup_t \frac{\tilde{I}_h(t)}{\tilde{N}_h(t)}$$

Rewriting the last expression we get

$$0 \geq \left(1 - R_{10}'^2\right) \limsup_t \frac{\tilde{I}_h(t)}{\tilde{N}_h(t)}$$

and using the condition that $R_{10}' \leq 1$, we have that $\limsup_t \frac{\tilde{I}_h(t)}{\tilde{N}_h(t)} \leq 0$. However, $\frac{\tilde{I}_h(t)}{\tilde{N}_h(t)} \geq 0$ so $\limsup_t \frac{\tilde{I}_h(t)}{\tilde{N}_h(t)} = 0$. On the other hand, substituting the other way around, we obtain similar results

$$\limsup_t \frac{\tilde{I}_v(t)}{\tilde{N}_v(t)} \leq \frac{\tilde{\beta}_h}{\mu_h+\alpha} \frac{\tilde{\beta}_v}{\mu_v} \limsup_t \frac{\tilde{I}_v(t)}{\tilde{N}_v(t)} = R_{10}'^2 \limsup_t \frac{\tilde{I}_v(t)}{\tilde{N}_v(t)}$$

and so $\limsup_t \frac{\tilde{I}_v(t)}{\tilde{N}_v(t)} = 0$. For the susceptibles, we have

$$\tilde{S}_h \leq \frac{\tilde{\Lambda}_h}{\mu_h} - \tilde{\beta}_h \int_0^t \tilde{S}_h(\tau) \frac{\tilde{I}_v(\tau)}{\tilde{N}_v(\tau)} e^{\mu_h(\tau-t)} d\tau$$

and similarly for $\tilde{S}_v$. Using the same arguments and methods as for the infected class, we obtain

$$\begin{aligned}
\limsup_t \tilde{S}_h &\leq \frac{\tilde{\Lambda}_h}{\mu_h} - \frac{\tilde{\beta}_h}{\mu_h} \limsup_t \tilde{S}_h(t) \frac{\tilde{I}_v(t)}{\tilde{N}_v(t)} \\
&= \frac{\tilde{\Lambda}_h}{\mu_h} - \frac{\tilde{\beta}_h}{\mu_h} \limsup_t \tilde{S}_h(t) \limsup_t \frac{\tilde{I}_v(t)}{\tilde{N}_v(t)} \\
&= \frac{\tilde{\Lambda}_h}{\mu_h}
\end{aligned}$$

and

$$\begin{aligned}
\limsup_t \tilde{S}_v &\leq \frac{K(r-\mu_v)}{r} - \frac{\tilde{\beta}_v}{r} \limsup_t \tilde{S}_v(t) \frac{\tilde{I}_h(t)}{\tilde{N}_h(t)} \\
&= \frac{K(r-\mu_v)}{r}
\end{aligned}$$

Therefore, the infection-free equilibrium is globally stable when $R'_{10} \leq 1$. □

C.2 Patch 2 (no migration)

We calculate the basic reproductive number R_{20} using the next generation operator method. This includes calculating the basic reproductive number for both the chagasic and the non-chagasic strains, which we will denote as R_{21} and R_{22}, respectively. We have

$$\begin{aligned}
R_{21} &= \sqrt{\frac{\beta_{h1}}{(\mu_h+\alpha)} \frac{\beta_{v1}}{\mu_v}} \\
R_{22} &= \sqrt{\frac{\beta_{h2}}{\mu_h} \frac{\beta_{v2}}{\mu_v}}
\end{aligned}$$

With this, we obtain the R_{20} for the whole patch as

$$R_{20} = \max\{R_{21}, R_{22}\}.$$

In the absence of migration, we can obtain four fixed points corresponding to the following situations: the infection-free equilibrium, denoted by E_{20}, in which there is no presence of either strain of *T. cruzi* in the patch; the endemic equilibrium in which strain 1 dominates (E_{21}); the endemic equilibrium in which strain 2 dominates (E_{22}); and finally, the coexistence equilibrium (E_{23}).

As in the previous section, we proportionalize the steady state conditions using the following:

$$\begin{aligned}
S_h^* &= (1-y_h-z_h) N_h^* \\
I_{h1}^* &= y_h N_h^* \\
I_{h2}^* &= z_h N_h^* \\
S_v^* &= (1-y_v-z_v) N_v^* \\
I_{v1}^* &= y_v N_v^* \\
I_{v2}^* &= z_v N_v^*
\end{aligned}$$

We computed the infection-free equilibrium, which is the following:

$$E_{20} : (S_h^*, I_{h1}^*, I_{h2}^*, S_v^*, I_{v1}^*, I_{v2}^*) = \left(\frac{\Lambda_h}{\mu_h}, 0, 0, \frac{K(r-\mu_v)}{r}, 0, 0\right)$$

Its existence is easily shown as well, because $\Lambda_h, \mu_h, K, r > 0$ and $r - \mu_v > 0$.

Similarly as for patch 1, we obtain the endemic equilibrium in which the chagasic strain dominates (E_{21})

$$E_{21}: \begin{pmatrix} 1-y_h-z_h \\ y_h \\ z_h \\ 1-y_v-z_v \\ y_v \\ z_v \end{pmatrix} = \begin{pmatrix} \frac{1}{R_{21}^2}+\left(1-\frac{1}{R_{21}^2}\right)\left(\frac{\mu_h+\alpha}{\mu_h+\alpha+\beta_{h1}}\right) \\ \left(1-\frac{1}{R_{21}^2}\right)\left(\frac{\beta_{h1}}{\mu_h+\alpha+\beta_{h1}}\right) \\ 0 \\ \frac{1}{R_{21}^2}+\left(1-\frac{1}{R_{21}^2}\right)\left(\frac{\mu_v}{\mu_v+\beta_{v1}}\right) \\ \left(1-\frac{1}{R_{21}^2}\right)\left(\frac{\beta_{v1}}{\mu_v+\beta_{v1}}\right) \\ 0 \end{pmatrix},$$

where

$$\begin{aligned} N_h &= \frac{\Lambda_h}{\mu_h+\alpha y_h}, \\ N_v &= K\left(1-\frac{\mu_v}{r}\right). \end{aligned}$$

The endemic equilibrium in which strain 2 dominates (E_{22}) is given by

$$E_{22}: \begin{pmatrix} 1-y_h-z_h \\ y_h \\ z_h \\ 1-y_v-z_v \\ y_v \\ z_v \end{pmatrix} = \begin{pmatrix} \frac{1}{R_{22}^2}+\left(1-\frac{1}{R_{22}^2}\right)\left(\frac{\mu_h}{\mu_h+\beta_{h2}}\right) \\ 0 \\ \left(1-\frac{1}{R_{22}^2}\right)\left(\frac{\beta_{h2}}{\mu_h+\beta_{h2}}\right) \\ \frac{1}{R_{22}^2}+\left(1-\frac{1}{R_{22}^2}\right)\left(\frac{\mu_v}{\mu_v+\beta_{v2}}\right) \\ 0 \\ \left(1-\frac{1}{R_{22}^2}\right)\left(\frac{\beta_{v2}}{\mu_v+\beta_{v2}}\right) \end{pmatrix}$$

where

$$\begin{aligned} N_h &= \frac{\Lambda_h}{\mu_h} \\ N_v &= K\left(1-\frac{\mu_v}{r}\right) \end{aligned}$$

We verified the existence of both endemic equilibrium points using the basic reproductive numbers. The existence of the equilibrium in which strain 1 dominates is given by the condition $R_{21} > 1$, which assures that $E_{21} > 0$. Similarly, the existence of the equilibrium in which strain 2 dominates is given by the condition $R_{22} > 1$, which assures that $E_{22} > 0$.

We prove that the coexistence equilibrium occurs only in the special case in which $R_{21} = R_{22} > 1$.

There are an infinite number of coexistence equilibrium points in patch 2 ($m = 0$) if and only if $R_{21} = R_{22} > 1$.

Proof. We go back to the proportionalized equations and the notation used before:

$$\begin{aligned} S_h^* &= (1-y_h-z_h)\,N_h^* \\ I_{h1}^* &= y_h N_h^* \\ I_{h2}^* &= z_h N_h^* \\ S_v^* &= (1-y_v-z_v)\,N_v^* \\ I_{v1}^* &= y_v N_v^* \\ I_{v2}^* &= z_v N_v^* \end{aligned}$$

From these definitions we see that it is sufficient to use four steady state equations.

$$\beta_{h1}\,(1-y_h-z_h)\,N_h y_v - \mu_h y_h N_h - \alpha y_h N_h = 0 \quad (89)$$

$$\beta_{h2}\,(1-y_h-z_h)\,N_h z_v - \mu_h z_h N_h = 0 \quad (90)$$

$$\beta_{v1}\,(1-y_v-z_v)\,N_v y_v - \mu_v y_v N_v = 0 \quad (91)$$

$$\beta_{v2}\,(1-y_v-z_v)\,N_v z_v - \mu_v z_v N_v = 0 \quad (92)$$

Note that (91) is linear in y_v and (92) is linear in z_v, so it is possible to solve for them in terms of y_h and z_h, obtaining

$$\begin{aligned} y_v &= \frac{\beta_{v1} y_h}{\beta_{v1} y_h + \beta_{v2} z_h + \mu_v} \\ z_v &= \frac{\beta_{v2} z_h}{\beta_{v1} y_h + \beta_{v2} z_h + \mu_v} \end{aligned}$$

If we now substitute these values in (89) and (90), we obtain the following expressions:

$$\begin{aligned} \frac{\beta_{h1}\beta_{v1}}{\mu_h + \alpha}(1 - y_h - z_h) &= \mu_v + \beta_{v1} y_h + \beta_{v2} z_h \\ \frac{\beta_{h1}\beta_{v1}}{\mu_h}(1 - y_h - z_h) &= \mu_v + \beta_{v1} y_h + \beta_{v2} z_h \end{aligned}$$

The left hand side of both equations should be equal, and in this case we obtain an infinite number of solutions for the system of equations. This means that we need

$$\frac{\beta_{h1}\beta_{v1}}{\mu_h + \alpha} = \frac{\beta_{h1}\beta_{v1}}{\mu_h}$$

and by dividing by μ_v in both sides we obtain the condition

$$R_{21} = R_{22}$$

which ends our proof □

This condition can also be restated posing conditions on the invasion reproductive numbers of each of the two strains.

The invasion reproductive numbers quantify the possibility of "invasion" by one strain in an environment in which the other strain is at a positive equilibrium [32]. In other words, the interpretation of these expressions follows the same line as that of the basic reproductive numbers: in our case they quantify the average number of secondary infections caused by introducing a vector infected with one of the strains into a population in which the other strain is endemic. If the invasion reproductive number of one strain is greater than 1, that means that the specific strain is capable of "invading" the other one. Note that in order for this analysis to make sense, we would also need the respective basic reproductive number for the invaded strain to be greater than one, because we are supposing that it is in its endemic equilibrium.

We obtained the invasion reproductive numbers for each of the strains. They are calculated using the same method which we use to calculate the basic reproductive number in general, the next generation operator method [32], but using the endemic equilibrium of the strain which is "under invasion" to evaluate the jacobian, instead of the disease free equilibrium. This is, we only consider the infected hosts and vectors of the strain that is invading as infective classes. We will denote the invasion reproductive numbers as R_{i1} and R_{i2} (for strain 1 when strain 2 is at an endemic equilibrium, and for strain 2 when strain 1 is at an endemic equilibrium, respectively). Each single strain equilibrium will exist if the respective invasion reproductive number is greater than 1. This is, if $R_{i1} > 1$, then we have the endemic equilibrium in which strain 1 dominates; similarly if $R_{i2} > 1$, we have the endemic equilibrium in which strain 2 dominates. Moreover, if both R_{i1} and R_{i2} are greater than 1, we may have a coexistence equilibrium point.

The results for the invasion reproductive numbers are given by the following expressions:

$$R_{i1} = \sqrt{\frac{\mu_h \beta_{h1} \beta_{v1}}{(\mu_h + \alpha)\beta_{h2}\beta_{v2}}}$$

$$R_{i2} = \sqrt{\frac{(\mu_h + \alpha)\beta_{h2}\beta_{v2}}{\mu_h \beta_{h1} \beta_{v1}}}$$

Scrutinizing the form of the invasion reproductive numbers, it can be seen that the two reproductive numbers are reciprocals of each other. The condition that both invasion reproductive numbers have to be greater than 1 for coexistence equilibrium to exist cannot be satisfied. Therefore, we have that the coexistence of the two strains is only found on the straight line of slope 1 (in the $R_{i1} - R_{i2}$ plane). In other words, we have coexistence at the

bifurcation line (where both invasion reproductive numbers are equal to 1). In our perspective, this result could be showing the importance of other methods of transmission, such as vertical transmission, in the possibility for coexistence of the two strains. This is because in [4], a similar model is analyzed for the cross-immunity problem with the difference that it takes into account vertical transmission of the disease in the hosts, and the author was able to impose conditions under which coexistence could occur. In our calculations, we obtained similar invasion numbers, but they limit the possibility of coexistence just to the bifurcation line (as we mentioned before). We think that in [4], in the presence of vertical transmission, there is a region of coexistence due to the fact that part of the host population is already infected and there is no actual competition for them.

C.2.1 Bifurcation analysis

Before we analyze the dynamics of equilibrium points on the stability diagram, we introduce a definition that we will use during the analysis of the steady states.

A steady state is called a type-k equilibrium point for a given set of parameter values if its corresponding Jacobian has exactly k eigenvalues with positive real parts.

For instance, in a two dimensional system, a *type-0* steady state is an asymptotically stable (sink) equilibrium point. All others are unstable equilibrium points (*type-1* for saddle and *type-2* for source). A *type-k equilibrium point* has a *(n-k)*-dimensional stable manifold and a k-dimensional unstable manifold. We now use this definition to gain insight into the type of steady states that exist in the different regions on the stability diagram shown in figure 29.

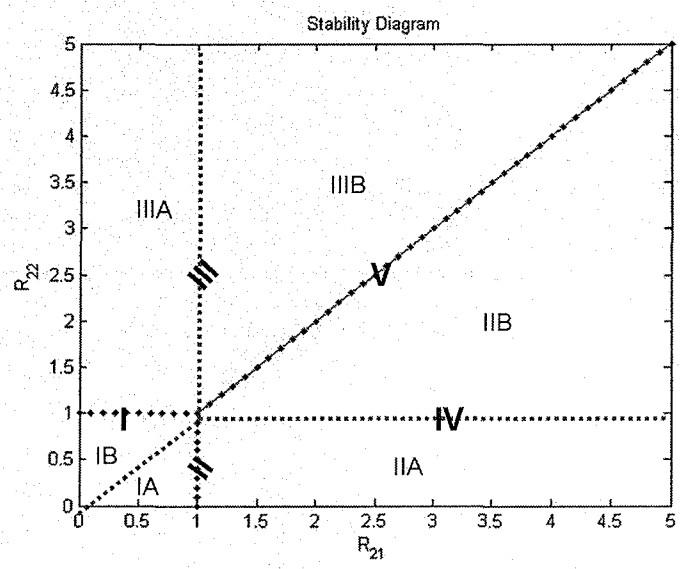

Figure 29: Stability Diagram for Bifurcations

The stability diagram above is divided into five different regions. The boundary lines shown on the stability diagram are the bifurcation threshold values satisfying various conditions imposed on the reproductive numbers. The boundaries $I - IV$ exhibit transcritical bifurcations and boundary V exhibits a bifurcation which we call a *switch bifurcation (degenerate transcritical bifurcation),* which will be discussed in detail later. E_{20}, E_{21}, and E_{22} are *type-0 equilibria* (locally stable) in regions (IA), (IIA and IIB), and ($IIIA$ and $IIIB$), respectively. In IA, the endemic equilibria E_{21} is a *type-1 steady state*, and E_{22} is a *type-2 steady state.* In IIA, the endemic equilibria E_{21} is a *type-2* while E_{22} is a *type-1 steady state.* Both of these equilibria are negative and therefore do not exist in our feasible state space (positive state space). From now on, we use sign superscript on the equilibrium (e.g.: E_{21}^{+}) to denote whether the steady state is in the feasible region (positive) or it is not (e.g.: E_{21}^{-}, negative). As we go through the boundary II, E_{20} becomes a *type-1 equilibrium*, E_{21}^{+} is now stable *(type-0)* and E_{22}^{-} is *type-2 equilibrium point* in region IIA. E_{21}^{+} remains stable in IIB, but the equilibrium E_{22}^{+} becomes

type-1 and E_{20} is *type-2*. The equilibria E_{20}, E_{21}^-, and E_{22}^+ are *type-1, type-2* and *type-0* in region $IIIA$, respectively. The E_{21}^+, E_{20} and E_{22}^+ are *type-1, type-2* and *type-0* in $IIIB$, respectively. All these transitions occur via transcritical bifurcations. In this model, only the positive steady states are valid because they are biologically interpretable. In summary, the region IA has only E_{20}, region IIA has E_{21} and E_{20}, region IIB and $IIIB$ have E_{20}, E_{21} and E_{22}, and region $IIIA$ has E_{20} and E_{22}.

	IA	IB	IIA	IIB	$IIIA$	$IIIB$
E_{20}	0	0	1	2	1	2
E_{21}	1	2	0	0	2	1
E_{22}	2	1	2	1	0	0
E_c	–	–	–	–	–	–

Table 15: Equilibrium type

To gain insight into the dynamics of the bifurcation that occurs on the line between E_{21} and E_{22} (which exists only when $R_{i1} = R_{i2}$), we use the properties of the type of equilibria that occur, which are summarized in table 15. But first we assume that there is no saddle-node bifurcation occuring on E_{21} or E_{22} when we go through boundary I or II, respectively. The setting of the problem can help us rule out the existence of a saddle-node bifurcation, because we can argue that the rest of the bifurcations that appear are transcritical [33]. In our model, there are two possible explanations that account for the gaining of an additional unstable dimension in E_{21} or E_{22} when they go through their respective boundary (I or II). The first explanation is that there is a transcritical bifurcation in one of the dimensions where E_c^- and E_{21} or E_c^- and E_{22} exchange dimensional stability. The second explanation is that there is a *one-to-one* transcritical bifurcation on the regions I and II, meaning that two simultaneous transcritical bifurcations occur on the boundary. However, we can rule this out when we look at the dimensional exchanges that occur on boundary III and IV (see Table 15). The only valid explanation is that the coexistence bifurcation line (boundary V) extends into region IA. However, since the negative steady states are not in our feasible region, this transcritical bifurcation is not observable. Using the assumption that only transcritical bifurcations occur on boundaries I, II, III, and IV, we can now try to understand the dynamics of the bifurcation on V. The bifurcation (switch or degenerate transcritical bifurcation) on the boundary (V) behaves like a co-dimension infinity bifurcation. The boundary endemic equilibria exchange their stability in a such a way that there are infinitely many stable non-isolated steady states connecting the two endemic equilibria at the moment of bifurcation. We use numerical calculation to show the existence of the coexistence equilibrium point on the bifurcation line where both invasion reproductive numbers are 1, and R_{21} and R_{22} are greater than 1 but equal. Satisfying these conditions, we calculated the steady states and showed that there is an infinite number of solutions where I_{h2}, I_{v1} and I_{v2} are dependent on I_{h1}, which is bounded by a constant. Our calculations show that there are three steady states before and after the bifurcation. However, at the bifurcation values, there are only two steady states, E_{20} and non-isolated coexistence equilibria E_c. Closer examination of the latter steady states shows that there are infinitely many solutions for the infection-state values.

C.3 The system with migration

In this case, we consider the parameter $m > 0$ for the cross-immunity patch, that is, we take into account the effects of migration. In order for migration to occur, we need to have the R_{10} (with migration) from patch one greater than one; if this is not true, the infection-free equilibrium E_{10} is stable and clearly there can be no infected vectors to migrate. However, when in patch 1 the chagasic strain reaches its endemic state, then there are enough infected vectors which can start migrating, creating a constant influx of vectors infected with the chagasic strain into patch 2 and changing its dynamics. To analyze the cross-immunity patch (patch 2), we can take patch 1 to its endemic equilibrium and use it in patch 2. This eliminates the existence of infection-free equilibrium. As a result, we have only two equilibrium points: the one where the chagasic strain dominates, and the coexistence equilibrium. It is not possible to have an infection-free equilibrium or an equilibrium where the non-virulent strain dominates, because there is a constant influx of infected vectors into this patch.

The basic reproductive number for patch 1 considering $m > 0$ is given by

$$R_{10} = \sqrt{\frac{\tilde{\beta}_h}{(\mu_h + \alpha)} \frac{\tilde{\beta}_v}{(\mu_v + m)}}$$

Note that this is almost the same expression which we presented before, but now it incorporates the constant migration term (m), so its biological interpretation remains the same.

To be consistent, we use the same notation as in the subsection for patch 1 with no migration: $\tilde{I}_h^* = x_h \tilde{N}_h^*$, $\tilde{I}_v^* = x_v \tilde{N}_v^*$. The endemic equilibrium for patch 1 with migration (E_{11}) results in the following

$$E_{11} : \begin{pmatrix} 1-x_h \\ x_h \\ 1-x_v \\ x_v \end{pmatrix} = \begin{pmatrix} \frac{1}{R_{10}^2} + \left(1-\frac{1}{R_{10}^2}\right)\left(\frac{\mu_h+\alpha}{\tilde{\beta}_h+\mu_h+\alpha}\right) \\ \left(1-\frac{1}{R_{10}^2}\right)\left(\frac{\tilde{\beta}_h}{\tilde{\beta}_h+\mu_h+\alpha}\right) \\ \frac{1}{R_{10}^2} + \left(1-\frac{1}{R_{10}^2}\right)\left(\frac{\mu_v+m}{\tilde{\beta}_v+\mu_v+m}\right) \\ \left(1-\frac{1}{R_{10}^2}\right)\left(\frac{\tilde{\beta}_v}{\tilde{\beta}_v+\mu_v+m}\right) \end{pmatrix}$$

where

$$\begin{aligned} \tilde{N}_h^* &= \frac{\Lambda}{\mu_h + \alpha x_h} \\ \tilde{N}_v^* &= K\left(1 - \frac{\mu_v + m x_v}{r}\right) \end{aligned}$$

The condition for the existence of this solution is $R_{10} > 1$. Also, it can easily be seen that this solution is consistent with the one we have for patch 1 without migration if we set $m = 0$. We can also see that $\tilde{N}_h^*$ remains unchanged by migration because we are assuming migration only for the vectors; clearly the vector population $\tilde{N}_v^*$ will decrease as migration increases.

We were also able to compute the endemic equilibrium for patch 2 with migration, in which strain 1 dominates (E_{31}, where the subscript 3 is used to denote patch 2 with migration). Using the same notation as before, in this case we have $z_h = 0, z_v = 0$,

$$\begin{aligned} y_v &= \frac{\beta_{v1} y_h + \frac{M}{N_v^*}}{\beta_{v1} y_h + \mu_v} \\ G(y_h) &= \left[\beta_{v1}\left(\beta_{h1} + \mu_h + \alpha\right)\right] y_h^2 \\ &\quad + \left[\beta_{h1}\frac{M}{N_v^*} + \left(\mu_h + \alpha\right)\mu_v - \beta_{v1}\beta_{h1}\right] y_h - \beta_{h1}\frac{M}{N_v^*} \\ &= 0 \end{aligned}$$

where we denote $M = m\tilde{I}_v^*$, and the total populations for hosts and vectors are the following:

$$\begin{aligned} N_h^* &= \frac{\Lambda_h}{\mu_h + \alpha y_h} \\ N_v^* &= K\left(1 - \frac{\mu_v}{r}\right)\left[\frac{1}{2}\left(1 + \sqrt{1 + 4\frac{M}{rK\left(1-\frac{\mu_v}{r}\right)^2}}\right)\right] \end{aligned}$$

From the equations above, we have that $G(y_h) = A y_h^2 + B y_h + C = 0$, where

$$\begin{aligned} A &= \beta_{v1}\left(\beta_{h1} + \mu_h + \alpha\right) \\ B &= \beta_{h1}\frac{M}{N_v^*} + \left(\mu_h + \alpha\right)\mu_v - \beta_{v1}\beta_{h1} \\ C &= -\beta_{h1}\frac{M}{N_v^*} \end{aligned}$$

so solving for y_h we have

$$y_h = \frac{-B \pm \sqrt{B^2 - 4AC}}{2A}$$

But $A > 0, C < 0 \Rightarrow \sqrt{B^2 - 4AC} > B^2 \Rightarrow B^2 - 4AC > |B|$, which means that we will always have 2 real roots: one positive and one negative. We neglect the negative root because it doesn't have biological meaning. We also verify that $0 < y_h < 1$ using the following observations: $G(0) = -\beta_{h1}\frac{M}{N_v^*} < 0$, and $G(1) = \left(\mu_h + \alpha\right)\left(\beta_{v1} + \mu_v\right) > 0$. So by the Intermediate Value Theorem the only positive root of G has to be in the interval between 0 and 1.

We also need the expression for y_v to be between 0 and 1. By its definition above, and because $0 < y_h < 1$, we will have $0 < y_v < 1$ if and only if $\frac{M}{N_v^*} \leq \mu_v$. We can assume this fact to be true because of two reasons. The first one is that we need $M \leq \mu_v N_v^*$, or else the total population of vectors will explode, this is, $N_v \to \infty$, as can be seen easily deduced by the original differential equation for patch 2:

$$\frac{dN_v}{dt} = rN_v\left(1 - \frac{N_v}{K}\right) - \mu_v N_v + M$$

This does not make sense in biological terms, because empirically we know that the vector population is not growing unboundedly. The second reason is that $M = m\tilde{I}_v^*$, and we are considering the term m to be small, such that it does not affect the behavior of R_{10} which should be greater than 1 in order for migration to occur (as has been stated before).

In order to determine if the non-virulent strain will be able to survive in patch 2 once migration exists, we calculate the invasion reproductive number for strain 2 when strain 1 is endemic (R_{i3}). In this case, we take the infected class to be $[I_{h2}, I_{v2}]$, and use the endemic equilibrium that we obtained previously for strain 1 to calculate it. The result is

$$R_{i3} = \sqrt{\frac{\beta_{h2}}{\mu_h}\frac{\beta_{v2}}{\mu_v}(1 - y_h)(1 - y_v)}$$

which we can actually rewrite using the basic reproductive number R_{22} and our definitions for y_h and y_v in E_{21} as

$$R_{i3} = R_{22}\sqrt{\left(1 - \frac{I_{h1}^*}{N_h^*}\right)\left(1 - \frac{I_{v1}^*}{N_v^*}\right)}$$

These proportions which appear in the invasion reproductive number come from the fact that the complete population of hosts (or of vectors) is not available for the two strains for infection.

When the conditions $R_{10} > 1$, $R_{20} > 1$, and $R_{i3} > 1$ are satisfied, we showed numerically that the coexistence equilibrium is stable. To do this, we fixed all the parameters except β_{h1} and used this to solve for $G(y_h) = 0$ and y_v. Then we plotted them as functions of β_{h1}. On Figure 30, it can be seen that the endemic equlibrium E_{31} is stable when β_{h1} is less than 2.25 and the coexistence E_{33} is stable for $\beta_{h1} > 2.25$. This change in stability happens via a transcritical bifurcation, as we can see in figure 30.

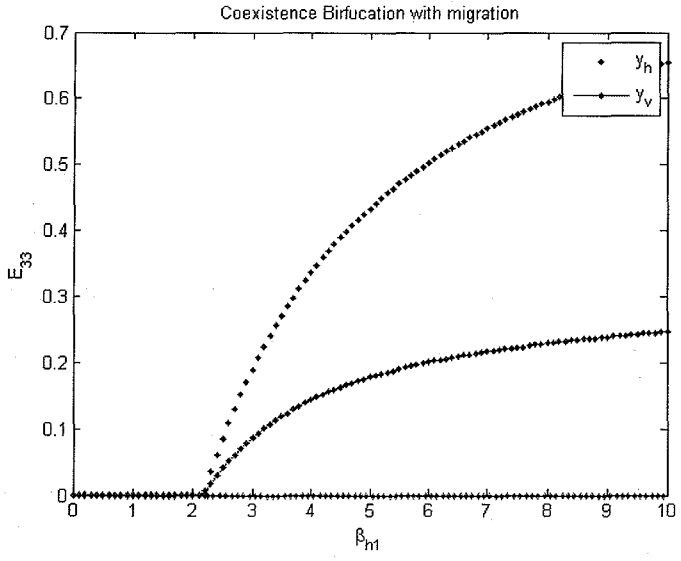

Figure 30: Transcritical Bifurcation with migration

C.4 The two patch system

In this section we look at the overall behavior of our system, which is dependent on the series of reproductive numbers that we computed.

We start by discussing the scenarios produced by our model when we take migration into account, that is, we have $m > 0$. The first consideration is that, in order for there to be migration, we need to have the basic reproductive number for patch 1 (before migration) greater than 1, i.e. $R'_{10} > 1$, because otherwise the infection-free equilibrium would be stable for this patch. Having $R'_{10} < 1$ would mean that the population of infected vectors goes to extinction, which would also make it impossible for migration to occur. This is why initially we need to have a stable endemic equilibrium for the chagasic strain in patch 1, which gives us the possibility of having infected vectors moving to the other patch.

In this case where we take migration into account, we have six different possibilities (or combinations) for equilibrium points in the system as a whole, which depend on the values of certain reproductive numbers. The first important thing to notice is that it is not possible to have the virulent strain persisting in patch 1 and not in patch 2, because there is then always a constant influx of infected vectors from patch 1 into patch 2. This accounts for the occurence of 6 and not 8 different options. Also, we cannot compute a basic reproductive number for patch 2 when there is an endemic equilibrium for strain 1 in patch 1, because we have no infection-free equilibrium in patch 2. In these cases, we use the invasion reproductive number for strain 2 when strain 1 is endemic (R_{i3}) for the analysis.

There are two main scenarios to consider for the system as a whole: when the basic reproductive number for patch 1 (with migration), R_{10}, is less than one, and when $R_{10} > 1$.

In the first case when R_{10} turns out to be less than 1, then patch 1 is in a stable infection-free equilibrium and no emigration. In this case, we are able to consider each of the patches separately because they are decoupled and migration cannot occur, because the population of infected vectors goes to extinction. That is, the analysis is reduced to the case in which $m = 0$. In patch 2 (now without immigration) we can have, under different conditions, an infection-free equilibrium, an endemic equilibrium for the virulent strain (where strain 1 is endemic), an endemic equilibria for the non-virulent strain (where this strain is endemic), and a coexistence equilibrium under very strict conditions.

The infection-free equilibrium (E_{20}) is locally stable when the basic reproductive number for this patch is less than one, that is, $R_{20} < 1$. The stability of the endemic equilibria or a coexistence equilibrium depends on the values of the invasion reproductive numbers. To have a stable endemic equilibria for strain 1 we need two conditions: the basic reproductive number for the virulent strain $R_{21} > 1$, and the invasion reproductive number for the non-virulent strain $R_{i2} < 1$. With the second condition, we assure that strain 2 cannot invade an environment in which strain 1 is endemic. Similarly, to have a stable endemic equilibrium for the non-virulent strain we need the conditions $R_{22} > 1$ and $R_{i1} < 1$. If both endemic equilibria are feasible, this is, $R_{21} > 1$ and $R_{22} > 1$, and both the invasion reproductive numbers are greater than 1, then we can have a coexistence equilibrium. However, as we mentioned before, in our model this only happens when $R_{i1} = R_{i2}$ because the invasion reproductive numbers turned out to be reciprocals of each other.

A different scenario takes place when $R_{10} > 1$. Here we take the value of m for the migration term to be small, in order not to affect the behavior of R_{10} (the reproductive number with migration, which is smaller because of the presence of m in the denominator) so that it is also greater than 1. If this changes, we would end up having an infection-free equilibrium in patch 1, invalidating our assumption for the existence of migration, as we stated above. In this case, we have an endemic equilibrium for the chagasic strain in patch 1, and for patch 2 we have two possibilities: either an endemic equilibrium for the chagasic strain, or a coexistence equilibrium. The assumption of m being small makes biological sense, because it represents the proportion of infected vectors that migrate from patch 1 into patch 2 in one year.

In summary, the six possibilities overall considering migration are:

- Infection-free equilibrium points for both Patch 1 and Patch 2, when $R_{10} < 1$ and $R_{20} < 1$.
- Infection-free equilibrium for Patch 1, and endemic equilibrium for the chagasic strain in Patch 2. This happens when $R_{10} < 1$, $R_{21} > 1$, and $R_{i2} < 1$.
- Endemic equilibrium for the chagasic strain in both patches, when $R_{10} > 1$, $R_{20} > 1$ and $R_{i3} < 1$ (because strain 2 cannot invade).

- Infection-free equilibrium for Patch 1, and endemic equilibrium for the non-chagasic strain in Patch 2, when $R_{10} < 1, R_{22} > 1$ and $R_{i1} < 1$.
- Infection-free equilibrium for Patch 1, and coexistence of the two strains in Patch 2, when $R_{10} < 1$, and $R_{21} = R_{22} > 1$ (or equivalently, $R_{i1} = R_{i2} = 1$).
- Endemic equilibrium for Patch 1, and coexistence in Patch 2, when $R_{10} > 1$, $R_{20} > 1$, and $R_{i3} > 1$.

D Analysis of a particular case

D.1 Parameter estimation

Notation	Value	Units	Reference
$\tilde{\Lambda}_h$	$1,240,250$	host / years	[22], [35]
$\tilde{\beta}_h$	0.5077	per year	from prevalence data in [27], [24]
μ_h	$(6.8)^{-1}$	per years	[28], [30]
α	0	per year	assumed
r	398.4	per year	[6]
K	346627	density per km	[24], [35]
$\tilde{\beta}_v$	0.5074	per year	from prevalence data in [27], [24]
Λ_h	$1,240,250$	# hosts / year	[22], [35]
μ_v	$(1.88)^{-1}$	per year	[14]
β_{h1}	0.5077	per year	from prevalence data in [27], [24]
β_{h2}	0.5324	per year	from prevalence data in [25], [26]
β_{v1}	0.5074	per year	from prevalence data in [27], [24]
β_{v2}	0.3451	per year	from prevalence data in [25], [26]

Table 16: Parameter values

For purposes of estimation, we consider Patch 1 to be a region from Mexico in which the chagasic strain of *T. cruzi* is endemic (Yucatan Peninsula). We consider Patch 2 to be a region of the southern United States (the eastern part of Texas going east all the way to Georgia) where strain 2 is present. We obtained data for the prevalence of hosts and vectors infected with *T. cruzi* in each of the patches. In the case of Patch 1 we consider a prevalence of infection of 54% in opossums [27], and of 34% in the vectors (*Triatoma dimidiata*) [24]. In the case of Patch 2, we consider a prevalence of infection of 45% among raccoons [25], [26], and of 22.6% in the vectors (*Triatoma sanguisuga*) [23].

First of all, we assume that $\tilde{\Lambda}_h = \Lambda_h$, and that the growth rate and the carrying capacity are the same in both patches. We also assume μ_h to be the same for both patches, and similarly for μ_v. This is because we are not taking into account the differences in environmental conditions between the two patches which may produce changes in the life span of either hosts or vectors. We only estimate these parameters very roughly. In order to estimate the death rate for hosts, we take into consideration the average between the life spans of raccoons and opossums, which is approximately 6.8 years [28, 30]; similarly for the death rate of the vectors, we use the average between that of *T. dimidiata* and *T. sanguisuga*, approximately 1.88 years [14]. Therefore, the death rates are the inverses of these quantities. To calculate the recruitment rate, we consider the two patches in such a way that their area is the same. Then we take the area of the patch, multiplied by the average frequency of raccoons and opossums in an area, and divided by the estimated average life span. For the growth rate of the vector population (r), we use their hatching rates expressed in years. Finally, the carrying capacity (K) is defined as the density of vectors per kilometer.

We then use the prevalence values mentioned above to estimate all the infection rates ($\tilde{\beta}_h$, $\tilde{\beta}_v$, β_{h1}, β_{h2}, β_{v1}, β_{v2}) as in [31]. By substituting the other parameters which we know, and these prevalence levels into the steady state equations for patch 1, we were able to obtain the values $\tilde{\beta}_h \approx 0.5077$ per year, and $\tilde{\beta}_v \approx 0.5074$ per year. We will use that $\tilde{\beta}_h = \beta_{h1}, \tilde{\beta}_v = \beta_{v1}$, because of the fact that they both refer to the virulent strain of *T. cruzi*. Similarly, we use the steady state equations for patch 2, considering strain 2 is endemic, and the prevalences we

obtained from the data, to solve for $\beta_{h2} \approx 0.5324$ per year, and $\beta_{v2} \approx 0.3451$ per year. The estimated values we obtained are listed in Table 16.

D.2 Discussion of results

Reproductive number	Value
R'_{10}	1.8128
R_{10}	1.6632
R_{21}	1.8135
R_{22}	1.5326
R_{20}	1.8135
R_{i1}	1.1841
R_{i2}	0.8445
R_{i3}	0.9908

Table 17: Numerical values for reproductive numbers when $m = 0.1$

We use the parameters in Table 16 to calculate numerical values for the basic and invasion reproductive numbers. We are considering the migration term to be $m = 0.1$. The results are listed in Table 17.

In this situation, we are in the scenario in which there is an endemic equilibrium in patch 1 for the chagasic strain and also an endemic for the chagasic strain in patch 2. It is interesting to note that the invasion number that we calculated in the presence of migration, R_{i3}, is very close to 1. This means that we are in a borderline where with a small perturbation would produce a situation in which we have a coexistence equilibrium.

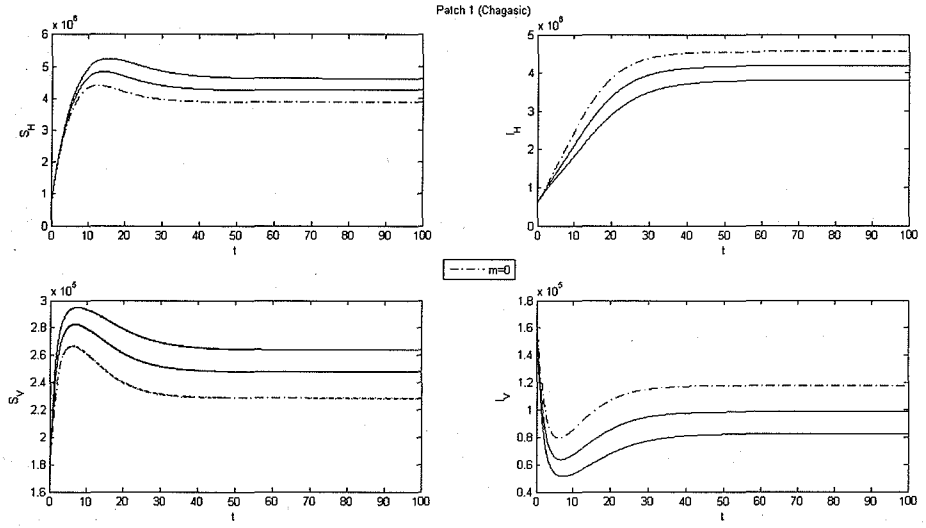

Figure 31: Time series for Patch 1

The interesting part of our model is the analysis of the two patches and the interaction between both when we add the migration term. We used the 10-dimensional model to analyze what happened in every case. We take into account the parameters which we found and estimated, and vary the parameter of migration m (per year). We want to know how the term m affects the behavior of the populations. As we have stated before, we need values for m such that $R_{10} > 1$ in order to avoid patch 1 going into infection-free equilibrium for patch 1. In these simulations, we consider the cases for $0 \leq m \leq 0.2$ per year.

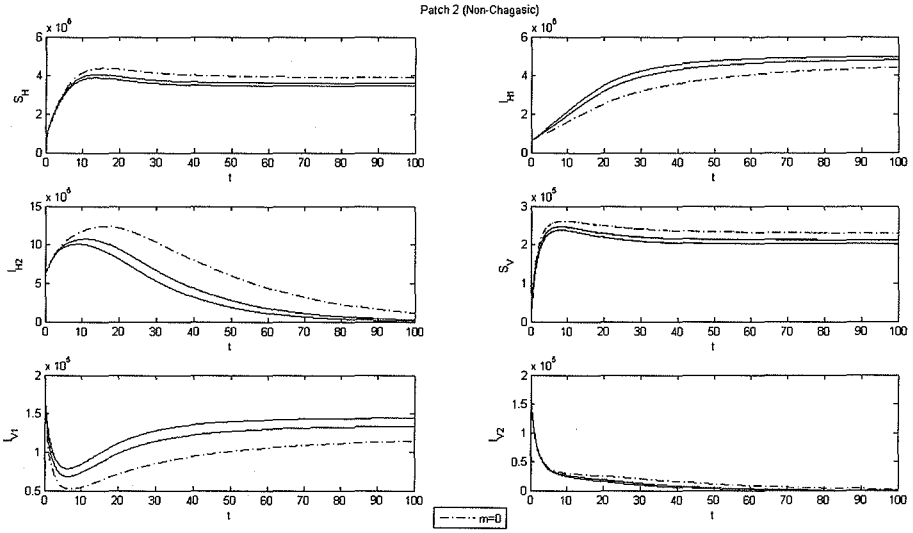

Figure 32: Time series for Patch 2

We can see their behavior in the time series plots (Figures 31 and 32). The dotted line denotes no migration, and the solid lines present a variety of migratory effects: m=0.1,0.2. In patch 1, the susceptible host and vector populations grow as the effect of migration increases, while the infected populations decrease, as expected because the infected vectors are leaving. In patch 2, we notice that the susceptible populations decrease significantly. Also, we see that the populations infected with the virulent strain increase while those infected with the non-virulent strain decrease. It can be seen that the most noticeable change in the dynamics of the populations occurs ten years from the initial time.

E Conclusions

Our analysis of the two-patch model has demonstrated that a population suffering from immigration of infected vectors with the virulent strain will always have some measure of the condition present within it. However, the initial presence of a competitive disease might serve as an ecological barrier against the invading malady. In the particular case of Chagas' disease, this barrier-like effect is due to the rigid requirements for coexistence. These requirements are based on the specific parameter values that describe the particular population that is being modelled. This can be seen clearly in our bifurcation analysis and on the stability diagram where the only possible region for coexistence is the line $R_{21} = R_{22}$. The same is true for our invasion numbers, which must also be equal in order for both strains to survive. This implies that coexistence is only possible if we assume that the strains are specialized, that is, if they target different hosts. Outside of these lines, the system will exhibit competitive exclusion. This implies that coexistence is possible when both strains have the same average number of secondary infections. This must hold true both in small presence of both strains as well as the endemic presence of one and small amount of the other. The rigid requirements for coexistence that we obtained suggest that other means of infection, such as vertical transmission and vector consumption, facilitate coexistence of both strains by reducing competition for susceptible hosts and vectors.

The commonality of this situation requires a further understanding of both strains and their ability to propagate. This might be the subject of further biological research. Given that the system does not meet the requirements for coexistence, the presence of the non-virulent strain will have one of two effects against a small short term migration of infected vectors. One of these occurs when $R_{i1} < 1$ in which case the population will exclude Chagas' in enough time after the cessation of migration. In this case, the non-virulent strain acts as a buffer against the invading disease. We will not have this buffer effect for the case when $R_{i1} > 1$. However, the presence of the competitive strain will act as a deterrent for the contagion of Chagas' disease, momentarily slowing down its invasion speed. However, this would be a topic for further mathematical research. It is also

important to note that there is not enough data in this area, and the one available is somewhat inconsistent, so further research efforts should be directed towards this.

It must be duly noted that these conclusions are feasible only with the particular assumptions that we take within our model. More compelling research projects might emerge by changing the pretext of the analysis. Incorporating things like vertical transmission and other forms of propagation would enrich the understanding about the contagious capabilities of Chagas'. Changing the migration term to a non-linear term, a parametric term depending on things like temperature or other environmental factors, periodic term like that exhibited in yearly migrations, incorporating a two-way migration to couple both patches or including host as well as vector migration, might expose new light on how animal migratory patterns affect the spread of diseases.

F Acknowledgements

The authors would like to thank Dr. Christopher Kribs-Zaleta, Dr. Fabio Sánchez, José Vega Guzmán, and Britnee Crawford for their invaluable help and supervision in this project. We would also like to thank Naala Brewer, Anuj Mubayi, Joaquín Rivera, and Faina Berezovsky for their comments and revisions on the manuscript, and Carlos Castillo-Chávez and Stephen Tennenbaum for the opportunity to participate in the program. This work was supported by The National Science Foundation (DMS-0502349), The National Security Agency (DOD-H982300710096), The Sloan Foundation, and Arizona State University, under the auspice of the MTBI/SUMS Summer Undergraduate Research Program.

References

[1] Lauria-Pires, L., Telxeira, A. R. L. (1997). *Protective Effect of Exposure to Non-virulent Trypanosoma cruzi Clones on the Course of Subsequent Infections with Highly Virulent Clones in Mice.* J. Comp. Path. Vol. 117. pp. 119-126.

[2] Kribs-Zaleta, C. (2006). *Vector Consumption and Contact Process Saturation in Sylvatic Transmission of T. cruzi.* Mathematical Population Studies, Vol. 13. pp.135-152

[3] Kribs-Zaleta, C. (2008). *Alternative transmission modes for Trypanosoma cruzi. in press*

[4] Kribs-Zaleta, C. (2008). *Cross-immunity and control in the transmission of Trypanosoma cruzi. in preparation*

[5] Pietrzak, S.M. and Pung, O.J. (1998). *Trypanosoma cruzi in racoons from Georgia.* J. Wildlife Diseases. Vol. 134 pp.132-136

[6] Martínez-Ibarra, J. A., Katthain-Duchateau, G. (1999). *Biology of Triatoma pallidipennis Stal 1945 (Hemiptera: Reduviidae: Triatominae) under Laboratory Conditions.* Memorias do Instituto Oswaldo Cruz, Vol.94-6. pp.837-839

[7] World Health Organization. *Disease Information.* From: http://www.who.int/tdr/diseases/chagas/diseaseinfo.htm Accessed July 2008.

[8] Oie, Institute for International Cooperation in Animal Biologist. (2006). *Chagas' disease.* pp. 1-8.

[9] Crawford, B. *The impact of vaccination and multiple types of HPV on cervical cancer. In press*

[10] Van den Driessche, P., Watmough. J. (2002). *Reproduction numbers and sub-threshold endemic equilibria for compartmental models of disease transmission.* Elsevier. Mathematical Bioscience. Vol. 180. pp. 29-48

[11] Rabinovich, J. E., Himschoot, P. (1990). *A population-dynamics simulation model of the the main vectors of Chagas' Disease transmission, Rhodnius prolixus and Triatoma infectans.* Ecological Modelling. Vol. 52. pp. 249-266.

[12] Dorn, P. L., Monroy, C. Curtis, A. (2007). *Triatoma dimidiata(Latreille, 1811): A review of its diversity across its geographic range and the relationship among populations.* Infection, Genetics and Evolution. Vol. 7. Pp. 343-352.

[13] Coll-Cárdenas, R, *et al.* (2004). *Active transmission of Human chagas Disase in Colima Mexico.* Mem. Inst Oswaldo Cruz. Vol.99(4). 363-368

[14] Velasco-Hernández, J. X. (1992). *A Model for Chagas Disease Involving Transmission by Vectors and Blood Transfusion.* Theoretical Population Biology. Vol. 46. pp. 1-31

[15] Martínez-Ibarra, J. A., *et al.*(2001). *Role of Two Triatoma (Hemiptera: Reduviidae: Triatominae) Species in the Transmission of Trypanosoma cruzi (Kinetoplastida: Trypanosomatidae) to Man in the West Coast of Mexico.* Mem Inst Oswaldo Cruz, Vol.96(2). pp. 141-144

[16] Añez, A. and Est, J.S. (1984). *Studies on Trypanosoma rangeli Tejera, 1920 II: Its effect on feeding behaviour of triatomine bugs.* Acta Tropica 41. pp. 93-95

[17] Alessandro, A., Mandel, S. (1969). *Natural infections and behaviour of Trypanosoma rangeli and T.cruzi in the vector Rhodnius prolixus in Colombia.* J. Parasit. Vol. 55. pp. 846-852

[18] Tobie, E. J. (1961). *Experimental transmission and biological comparision of strains of Trypanosoma rangeli.* Exp. Parasit. Vol. 11. pp. 1-9

[19] Reinhard, K., Finck, M., T., Skiles, J. (2003). *A Case of Megacolon in Rio Grande Valley As a Posible Case Chagas Disease.* Mem Inst Oswaldo Cruz, Vol. 98(Suppl. I). pp.165-172

[20] Nuño, M.,Chowell, G., Wang, X., Castillo-Chavez, C. (2007). *On role of cross immunity and vaccines on the survival of the less fit flu-strains.* Theoretical Population Biology. Vol. 71. 20-29.

[21] Hall, C., A., Polizzi, C., Yabstaley, M. J., and Norton, T. M., (2002). *Trypanasoma Cruzi Prevalence and Epidemiologic Trends in Lemurs on St.Catherine, Georgia. J.Parasitol.* Vol. 93.(1). 93-96.

[22] Conner C. Mark. (1983). *Scent-Station Indices as Measures of population Abundance for Bobcats, Raccoons, Gray Foxes, and Opposums.* Wildlife Society Bullentin, Vol. 11. No.2. pp. 146-152.

[23] Burkholder, J.E., Allison, T.C., Kelly, V. P. (1980). *Tryponosoma Cruzi (Chagas) (Protozoan: Kiretoplastida) In Invertebrate, Reservior and Human Host Of The Lower Rio Grande Valley of Texas.* J.Parasitol. Vol. 66(2). pp. 305-311.

[24] Dumontiel, E., *et al.* (2002). *Geographic Distribution of Triatoma Dimidiata and Transmission Dynamics of Trypanosoma Cruzi in the Yucatan Peninsula of Mexico.* Am J Trop Med Hyg. 67(2). pp. 176-183.

[25] Pietrzalk, S. M., Pung, O. J. (1998). *Trypanosomiasis in Raccoons from Georgia.* Journal of Wildlife Diseases. Vol. 34(1). pp. 132-136.

[26] Yabsley, M. J., Noblet, D. G. (2002). *Seroprevalence of Trypanosoma Cruzi in Raccoons from South Carolina and Georgia.* Journal of Wildlife Diseases. 38(1). pp. 75-85.

[27] Ruiz-Piã, H. A., Cruz-Reyez, A. (2002). *The Opossum Didelphis virginiana as a Synanthropic Reservoir of Trypanasoma Cruzi in Dzidzilché, Yucatán, México.* Mem Inst Oswaldo Cruz. Vol. 97(5). pp. 613-620.

[28] University of Michigan Museum of Zoology. (2008). *Procyon lotor.* http://animaldiversity.ummz.umich.edu/site/accounts/information/Procyonlotor.html.

[29] Cherif, A. (2007). *Integro-differential method in global stability of Hamiltonian Politics: Modeling the dynamics of sociopolitical Instability.* IPCP2007. Cornell University, Ithaca, NY

[30] University of Michigan Museum of Zoology. (2008). *Neotoma floridana.* http://animaldiversity.ummz.umich.edu/site/accounts/information/Neotomafloridana.html

[31] Mubayi, A., Wang, X., et al. *Types of Drinkers and Drinking Settings: Application of a Mathematical Model.* Preprint.

[32] Zhang, P., et al. (2007). *Evolutionary implications for interactions between multiple strains of host and parasite.* J. Theoretical Biology 248, pp. 225-240.

[33] Guckenheimer, J., Holmes, P. (1984). *Nonlinear oscillations, dynamical systems, and bifurcations of vector fields.* Springer-Verlag.

[34] Lambert, R.C., Kolivras, K.N., et al. (2008). *The potential for emergence of Chagas disease in the United States.* Geospatial Health 2(2): in press.

[35] Wikipedia, the free encyclopedia. (2008). http://en.wikipedia.org/wiki.